HHS Public Access

Author manuscript

Biopharm Drug Dispos. Author manuscript; available in PMC 2022 May 01.

Published in final edited form as:

Biopharm Drug Dispos. 2021 May ; 42(5): 191–203. doi:10.1002/bdd.2266.

Across-species meta-analysis of dexamethasone pharmacokinetics utilizing allometric and scaling modeling approaches

Dawei Song, **William J Jusko**

Department of Pharmaceutical Sciences, School of Pharmacy and Pharmaceutical Sciences, State University of New York at Buffalo, Buffalo, New York, USA

Abstract

The pharmacokinetic (PK) parameters of dexamethasone (DEX) in 11 species were collected from the literature and clearances (CL) assessed by basic allometric methods, and concentration–time course profiles were fitted using two PK models incorporating physiological or allometric scaling. Plots of log CL vs. log body weights (BW) correlated reasonably with R^2 = 0.91, with a maximum ratio of actual to fitted CL of 6 (for pig). A minimal physiologically-based pharmacokinetic (mPBPK) model containing blood and two lumped tissue compartments and integrated utilization of physiological parameters was compared to an allometric two-compartment model (a2CM). The plasma PK profiles of DEX from 11 species were analyzed jointly, with the mPBPK model having conserved partition coefficients (K_p), physiologic blood and tissue volumes, and species-specific CL values. The DEX PK profiles were reasonably captured by the mPBPK model for 9 of 11 species in the joint analysis with three fitted parameters (besides CL) including an overall tissue-to-plasma partition coefficient of 1.07. The a2CM with distribution CL and central and peripheral volumes scaled allometrically fitted the plasma concentration profiles similarly but required a total of six parameters (besides CL). Overall, the literature reported that DEX CL values exhibit moderate variability (mean = 0.64 L/h/kg; coefficient of variation = 105%), but distribution parameters were largely conserved across most species.

Keywords

clearance; dexamethasone; interspecies scaling; physiological pharmacokinetics

1 | INTRODUCTION

Dexamethasone (DEX) is a synthetic glucocorticoid used therapeutically in animals and humans to treat inflammation, allay allergic reactions, assess adrenal function, improve lung function in premature infants, and treat various cancers (Braat et al., 1992; Charles et

Correspondence: William J Jusko, Department of Pharmaceutical Sciences, School of Pharmacy and Pharmaceutical Sciences, State University of New York at Buffalo, 404 Pharmacy Building, Buffalo, NY 14214-8033, USA. wjjusko@buffalo.edu.

CONFLICT OF INTEREST

The authors declare that there are no conflicts of interest.

SUPPORTING INFORMATION

Additional supporting information may be found online in the Supporting Information section at the end of this article.

al., 1993; Li et al., 2012). The drug has moderate size (molecular weight = 392.5 g/mol), lipophilicity (log P = 1.83), and solubility (89 mg/L at 25°C) (DrugBank database). It was found to have a moderate volume of distribution (V_{ss} = 63 L) and half-life ($t_{1/2\beta}$ = 3–4 h) in humans (Mager et al., 2003; Tsuei et al., 1979). The pharmacokinetics (PK) of DEX has not been systematically assessed across various species, although we recently developed a full physiologically-based pharmacokinetic (PBPK) model for DEX in rats (Song et al., 2020). One application of a generic PBPK model parameterized the system for human physiology. DEX was one of many compounds in the training set, but it was not possible to discern specific parameter values used for DEX (Brightman et al., 2006). The human PBPK of DEX was simulated in pregnant women using the Simcyp Simulator (Certara, Princeton, NJ) (Ke & Milad, 2019).

Allometric scaling is often used to interrelate drug doses and PK parameters from animals to man. It is based on energy requirements and rates of physiological processes being closely associated with body size (Boxenbaum, 1982). Traditional basic allometric scaling in PK often involves two steps. First, parameters (such as clearances [CL] and volumes) are calculated using classical compartmental or noncompartmental analysis (NCA) methods. Then parameters from several species are used to extrapolate or compare to humans via simple allometric scaling (plotting $Y = a \times BW^b$ as $\log Y = \log a + b \times \log BW$) in relation to body weights (BW). This approach has been extended to assessing similar relationships for the semiphysiological parameters of two-compartment models (2CM) (Lepist & Jusko, 2004). However, parameters computed by these methods utilize little information about physiology among an array of species (Hall et al., 2012). Traditional basic interspecies allometric scaling is empirical and does not perform well for many drugs.

The intrinsic CL of antipyrine were able to be scaled across 15 mammalian species using body and brain weights partly owing to the extensive data that were available, as this compound was once a common biomarker for rates of drug metabolism (Boxenbaum & Fertig, 1984). An assessment of 44 drugs across veterinary and laboratory species observed that “clearance showed weak allometric correlations with weight across species” and focused on scaling half-life (Riviere et al., 1997, p. 453). Comprehensive assessments of basic allometric scaling methods involved 61 small molecule compounds that demonstrated a range of b values for CL from 0.3 to 1.2 with a central b value near 0.75 (Tang & Mayersohn, 2005). Later, 81 compounds were shown to exhibit a range of b values of 0.443–1.63 across species (Huh et al., 2011).

PBPK models include biological subsystems such as blood, lymphatics, elimination mechanisms, and structures of diverse tissues and organs. The PK of drugs is interpreted based on integrated physiology and in vivo mechanisms. Species-specific parameters (i.e., the mass/volumes and blood flow rates of tissues) and drug-specific information (i.e., tissue-to-plasma partition coefficients, protein binding parameters) are used in tandem (Meno-Tetang et al., 2006). However, building a full PBPK model requires measured or calculated drug concentrations in various tissues along with measured or extrapolated renal excretion and metabolic information.

Minimal physiologically-based pharmacokinetic (mPBPK) models inherit and lump major physiologic attributes from whole-body PBPK models (Cao & Jusko, 2012). They offer a simple and sensible modeling approach to incorporate physiological elements into a PK analyses when only plasma data are available. Integrating allometric scaling of CL into a mPBPK model can be useful for PK interspecies scaling. The across-species fitting and scaling of moxifloxacin (Cao & Jusko, 2012) and several monoclonal antibodies (Zhao et al., 2015) have been performed successfully using mPBPK models.

Available PK data for DEX were collected in 11 species, often for multiple studies for some species. Diverse PK data for DEX in many healthy human studies were also found. A mPBPK model with blood and two physiological lumped compartments was used to jointly analyze DEX PK across the species. An extended allometric two-compartment model (a2CM) where all distribution parameters were allometrically scaled was employed. We sought to: (1) provide a review of the literature regarding DEX PK and metabolism in various species, (2) assess DEX PK across all available species using traditional basic allometric approaches, and (3) test whether distribution parameters for DEX generalize across species based on joint fittings of time courses of plasma concentrations comparing mPBPK and a2CM models. This effort also provided insights into issues encountered when trying to assemble complete information about one drug from all available literature sources.

2 | METHODS

2.1 | Basic allometric scaling

Values of pharmacokinetic parameters such as plasma CL and steady-state volume of distribution (V_{ss}) were obtained from literature sources for as many species as could be found. If not reported directly, these parameters were either calculated from available descriptors or obtained by NCA from the plasma concentration vs. time profiles. The latter were regenerated from the published graphs by digitization (Rodionov, 2000).

2.2 | mPBPK model integrated with allometric scaling

The mPBPK model structure is shown in Figure 1. Blood and two lumped tissue compartments were assumed. The model equations and initial conditions are:

$$R_b \cdot \frac{dC_p}{dt} = Q_{co} \cdot f_{d1} \cdot \frac{R_b \cdot C_{t1}}{K_p \cdot V_b} + Q_{co} \cdot f_{d2} \cdot \frac{R_b \cdot C_{t2}}{K_p \cdot V_b} - \frac{R_b \cdot C_p}{V_b} \cdot ((f_{d1} + f_{d2}) \cdot Q_{CO} + CL) R_b \;\; C_p(0) = \frac{\text{Dose}}{V_b} \tag{1}$$

$$\frac{dC_{t1}}{dt} = \frac{Q_{co}}{V_{t1}} \cdot f_{d1} \cdot \left(R_b \cdot C_p - \frac{R_b \cdot C_{t1}}{K_p} \right) \;\; C_{t1}(0) = 0 \tag{2}$$

$$\frac{dC_{t2}}{dt} = \frac{Q_{co}}{V_{t2}} \cdot f_{d2} \cdot \left(R_b \cdot C_p - \frac{R_b \cdot C_{t2}}{K_p} \right) \;\; C_{t2}(0) = 0 \tag{3}$$

where C_p is the DEX concentration in plasma, C_{t1} is the DEX concentration in one lumped tissue (V_{t1}), C_{t2} is the DEX concentration in the second lumped tissue (V_{t2}), Q_{co} is cardiac blood flow, f_{d1} and f_{d2} are the fractions of Q_{co} accessing V_{t1} and V_{t2}, K_p is the plasma tissue partition coefficient, R_b is the blood to plasma ratio, V_b is blood volume, and CL is the species-specific CL. As in full PBPK models, blood flows and blood/plasma ratios are used in the model equations.

This model features physiological parameters and restrictions. The blood volumes for most species were adapted from one source (Wolfensohn & Lloyd, 2003), except for chicken (Kotula & Helbacka, 1966), camel (Banerjee & Bhattacharjee, 1963), and man (Brown et al., 1997). The information on the blood to plasma ratio was found to be 0.72 in rat (Song et al., 2020), 1.34 in monkey, and 0.95 in man (Akabane et al., 2010). The R_b for all species was assumed to be the average, which was 1.0. With conversion by R_b, the observed plasma PK data from the literature were fitted. The cardiac output flows were allometrically calculated for each species (Brown et al., 1997) as:

$$Q_{CO} = 0.275 \cdot BW^{0.75} \tag{4}$$

The mean BW (in kg) reported in each publication that had PK data was used. The tissue volume fractions for the compartments (F_t) were related to BW by assuming 1 g/ml tissue density across all species:

$$V_{t1} = (BW - V_b) \cdot F_t \tag{5}$$

$$V_{t2} = (BW - V_b) \cdot (1 - F_t) \tag{6}$$

$$f_{d1} + f_{d2} \leq 1. \tag{7}$$

The fitted parameters were F_t and f_{d1}, while f_{d2} is a secondary parameter. The F_t term allows separation of the body mass into two major components, ostensibly the highly and poorly perfused tissues. DEX is a small, moderately lipid-soluble drug and is thus assumed to permeate all body tissues, which accounts for the use of BW in these equations as in most full PBPK models. Parameter definitions are also provided in Table 1.

2.3 | a2CM

The a2CM is depicted in Figure 2. The equations used were:

$$\frac{dC_{cen}}{dt} = \frac{CL_D}{V_{cen}} \cdot (C_{per} - C_{cen}) - \frac{CL}{V_{cen}} \cdot C_{cen} \quad C_{cen}(0) = Dose/V_{cen} \tag{8}$$

$$\frac{dC_{per}}{dt} = \frac{CL_D}{V_{per}} \cdot (C_{cen} - C_{per}) \quad C_{per}(0) = 0 \tag{9}$$

where C_{cen} and C_{per} are the DEX concentrations in the central/plasma (V_{cen}) and peripheral volumes (V_{per}) with elimination (CL) and distribution (CL_D) clearances. Species-specific CL values were used and all other parameters expressed as $a \cdot BW^b$. All species were given the same fitted a_1 and b_1 (intercept and exponent values) of V_{cen}, a_2 and b_2 (for V_{per}), and a_3 and b_3 (for CL_D). All parameters are defined in Table 2.

2.4 | Model fittings

The maximum likelihood method in ADAPT5 was used to fit the models (D'Argenio & Schumizky, 2009). The variance model was:

$$V_i = (\sigma_1 + \sigma_2 \cdot Y_i)^2 \quad (10)$$

where V_i represents the variance of the ith data point, Y_i is the ith model prediction, and σ_1 as well as σ_2 are variance model parameters, which were estimated together with system parameters. The performance of the models was evaluated by goodness-of-fittings, visual inspection, Akaike Information Criterion (AIC), and coefficient of variation (CV%) of the estimated parameters. The ADAPT model codes for enacting the mPBPK and a2CM are provided in the Supporting Information Materials. The NCA assessments were performed using the Phoenix 8.1 software (Certara). All figures were created using GraphPad Prism 7.04 (GraphPad Software, San Diego, CA).

3 | RESULTS

The PK parameters of DEX found for 11 species are listed in Table 3. There were multiple studies with PK data available for some of the species. Studies of DEX PK for IV doses in various healthy adult human studies are listed in Table 4. The plasma concentration vs. time data for rats and man were from in-house studies (Mager et al., 2003; Samtani & Jusko, 2005a, 2005b) and all others were either from published tables or digitized.

For species with multiple studies, the PK data selected for modeling were based on the closeness of weight-normalized dose to other species, richness of sampling timepoints, details of study design, and alignment of CL values with basic allometric fitting. The literature-reported typical CL values were plotted vs. BW (log/log) across 11 species to test whether there was a simple allometric relationship. Only one value per species was included, which ensured equal weighting of the CL value from each species. As shown in Figure 3, basic allometry yields reasonable correlation of CL with BW (R^2 = 0.91). As is typical with these types of log/log graphs, the concordance of the actual vs. least-squares fitted values appears good because of the wide spread of log BW, but the ratio of actual CL to calculated values from the allometric equation is as large as 6 (for pig). Comparisons of the published, NCA, and allometrically regressed CL values shown in Table 3 depict their similarities and differences. Note that the NCA values came from digitized graphs and may not reflect published mean values of CL. Assessing the contribution of maximum life span and brain weight (Mahmood, 1998) to this type of regression did not result in any improvements. Because the CL value determines the area under the curve (AUC), there is little chance of improving upon the fitting of the time course of plasma concentrations in applying a more complete PK model when the basic allometric fitting for CL is divergent from the regression

value. Thus, the subsequent mPBPK and a2CM fittings were performed five ways: by using the CL obtained by NCA from individual digitized curves, by fitting data for each species with the mPBPK and 2CM models, and by fitting individual CL values jointly with the joint distribution parameters of the mPBPK and a2CM models. Only the latter will be shown, as it functioned best. All CL values are based on the same data with the assumption that CL occurs from plasma. With such individualized CL values, the modeling questions then become, "How similar are the distribution kinetics of DEX across species?" and "How do the mPBPK and a2CM approaches compare in resolving distribution parameters across species?"

The DEX PK profiles of the 11 species were jointly analyzed using the mPBPK model with separately fitted CL for each species, as shown in Figure 4. This model utilizes blood and tissue spaces proportional to BW and distribution rates governed by cardiac output, which is also related to species mass. Along with the current model structure, the mPBPK model with one tissue compartment (one K_p) or two tissue compartments (with differing K_p values) were assessed and they did not work as well as the present approach. The PK profiles were reasonably captured, except for pig and rabbit, many extremely well. The model-fitted distribution parameters are listed in Table 1 and jointly fitted CL for each species in Table 5. In the preliminary fitting, the f_{d1} and f_{d2} values were allowed to float but summation of these parameters was very close to 1.0 (>0.9999), and thus $f_{d1} + f_{d2}$ was fixed to 1.0 and only f_{d1} was estimated while f_{d2} became a secondary parameter. The K_p value is 1.07, which is similar—as expected—to most of the model-determined V_{ss} values as L/kg listed in Tables 3 and 4. Tissue 1 has the smaller volume (0.26·BW), receiving 85% of Q_{co}, while tissue 2 has a larger volume (0.70·BW) receiving 15% of Q_{co}. For mouse, the first-order absorption rate constant (*ka*) was fixed to 5 h^{-1} for the observed rapid absorption and the bioavailability (*F*) was fixed to 0.86, as reported in rat (Samtani & Jusko, 2005a, 2005b). In spite of the divergent fittings of two species, the CV% values for the mPBPK model parameters were all less than 8% (Table 1). The fittings and parameters changed very little when the profiles for rabbit and pig were not included. These two species exhibited the most divergent NCA and fitted CL and V_{ss} values from those originally reported compared to all other species (Tables 3 and 5).

Figure 5 shows the fittings of DEX plasma concentration vs. time curves for the same 11 species using the joint a2CM. In applying this model, the distribution parameters V_{cen}, V_{per}, and CL_D all utilize an allometric scaling relationship with BW ($Y = a \times BW^b$). The estimated slopes (*a*) and exponents (*b*) of the three parameters that were generated in Figure 5 are listed in Table 2 and fitted CL values in Table 5. The largest CV% value is 52.85%, but the others were very small, indicating reasonable model performance. The scaling exponents (*b*) ranged 0.88 to 1.13 indicating close, but not exact, direct proportionality to BW. The fittings and parameters changed very little when the profiles for rabbit and pig were not included, possibly because their PK diverged from the rest in opposite directions.

A comparison of CL values obtained by different methods is provided in Table S1, whereas fitted parameters for each individual species using the mPBPK model are in Table S2 and the 2CM model in Table S3. The NCA and model-fitted CL values are usually close to the reported values, but differ sometimes. Otherwise, the two mPBPK and two 2CM fitted

values are in concordance except for pig and rabbit, where these values also differ from reported values. When the mPBPK model is applied to each species individually, the array of PK parameters exhibits moderate variability. For example, K_p has a mean of 1.09 and CV% of 50.22 when assessed in each species, while the joint fitting yields a K_p = 1.07 with CV% = 1.93. For the 2CM, the V_{ss} averages 1.18 L/kg with CV% of 56.8 for individual fittings, whereas the scaling intercepts for V_{cen} (CV% 14.8) and V_{per} (CV% 17.2) add up to a V_{ss} of 1.25 L/kg.

In addition to the presented data for 11 species, oral dose data for DEX in pregnant sheep were found (Schmidt et al., 2019) without reported PK parameters. Our PK analysis of the data provided by the authors produced a mean CL/F of 0.98 L/h/kg. This value is much higher than most other species (Table 3), but this might be due to incomplete bioavailability (F) and/or faster metabolism (CL) owing to pregnancy.

4 | DISCUSSION

DEX is a therapeutic agent in human and veterinary medicine and thus has been studied in many species. We used PK data from 11 species to assess if CL scales to BW and whether tissue distribution parameters of DEX in those species can be generalized. Although we chose to use one representative CL value and one PK profile per species to allow for equal weighting, alternative approaches might be to stage different levels of analyses ranging from using mean values from all known studies to using individual subject data from all studies, if available. These methods would produce a cloud of values in both the Y- and X-directions in a graph such as Figure 3.

4.1 | Model comparison

The mPBPK and a2CM models for DEX utilized species-specific fitted CL values in the joint fittings, as allometric scaling of this parameter was reasonable but erratic (Figure 3 and Table 3). The mPBPK model used known or expected physiological parameters for blood volume, cardiac output, and BW for all species, while the a2CM model only includes BW for each species. The DEX PK profiles of most species were well-captured with both models. In their basic structures, the two PK models have analogous features with the mPBPK model, having blood and V_{t1} spaces that resemble the central compartment of the a2CM, the V_{t2} space that resembles the a2CM peripheral compartment, and $f_{d2} \times Q_{co}$ resembling CL_D. The volume parameters of the 2CM are often considered hypothetical spaces, while the mPBPK model provides a rationalization of volumes as lumped real tissues (Cao & Jusko, 2012). The jointly fitted CL values for the two methods were usually very close, although utilizing blood volume as the initial distribution space (as in full PBPK models) adds an early exponential phase and a slightly higher AUC for the mPBPK model, producing a slightly lower CL (Table 5), as expected (Cao & Jusko, 2012). Both models produced visually similar fittings, with discrepancies for pig and rabbit (Figures 4 and 5). The CV% values for fitted parameters were comparable and AIC values were quite similar (Tables 1 and 2). Operation of the mPBPK model requires greater insight and modeling skill than the 2CM. However, it is awkward to use a table of allometric coefficients to describe the distribution parameters of a drug across species, while it is easier to use parameters

from the mPBPK model to make such generalization. The mPBPK model produced a K_p value that matches most of the V_{ss}/BW values for DEX in various species, including many different studies in man (Tables 3 and 4). The tissue-average K_p value of 1.07 was intermediate to the array of tissue K_p values directly measured in PBPK studies in rats (Song et al., 2020). The latter study had DEX given subcutaneously and found a CL value of 0.198 L/h/kg, similar to the others in Table 3. DEX exhibits perfusion rate-limited distribution, as the f_{d1} and f_{d2} values add up to 1.0. With analyzing only plasma PK data, in comparison to the a2CM, the mPBPK modeling approach offers better insights on how DEX is distributed into tissues, answers whether distribution properties are conserved across species, and allows easier comparison to full PBPK models.

4.2 | Species PK comparisons

In performing this literature search and review, it was interesting to find several different publications that describe DEX PK in the same species. As shown in Table 3, similar CL and V_{ss} parameters were found across five studies in rats and across five studies in horses. Another study in horses (Toutain et al., 1984) reported a much higher CL, but collected blood for only 3 h. The most definitive study in horses was one that used liquid chromatography with mass spectroscopy/mass spectroscopy (LC-MS/MS) to assess DEX PK out to 96 h (Knych et al., 2020). There were two studies in monkeys with similar CL values and two studies in dogs with differing CL and V_{ss} values. Differences among studies in the sex of animals, doses of DEX, analytical methods, sampling times, and duration of sampling are possible reasons for variability in PK parameters. Another reason relates to the dosing of DEX free alcohol vs. DEX sodium phosphate. The latter contains 76% DEX and it was not always clear which moiety the publications used as the basis for the dose for calculation of PK parameters. Furthermore, DEX sodium phosphate is a salt/ester prodrug that exhibits short-lived PK (half-life 5.4 min in man) on its own. Rapid de-esterification also occurs in rat, rabbit, and dog (Kitagawa et al., 1972). Some studies (Hochhaus et al., 2001; Miyabo et al., 1981; Samtani & Jusko, 2005a, 2005b) used stabilizers to prevent postcollection in vitro hydrolysis of the ester in order to measure actual DEX in plasma, while many did not. It was observed in a PK study in rats using IV DEX phosphate sodium that the extremely rapid inactivation of the prodrug allows an assumption of instantaneous input of DEX for PK analysis (Samtani & Jusko, 2005a, 2005b). An early study of the PK of separately measured DEX and DEX phosphate sodium showed that the AUC of the latter was 19.9% of that of DEX, although DEX was measured by radioimmunoassay (RIA) only out to 24 h (Rohdewald et al., 1987). Species differences in esterase and hydrolase activities sometimes exist (Bahar et al., 2012), but we were unable to find systematic studies of phosphatase activity across species.

Many of these considerations also pertain to comparisons across the 13 studies that provided DEX PK in healthy adult subjects (Table 4). Other data can be found in the literature for DEX PK for nonparenteral doses, in different diseases, and part of drug interaction studies. The PK of DEX does not appear to differ with sex in man, although it does in rats (Song et al., 2020), and its PK is linear (Hare et al., 1975; Rohdewald et al., 1987). There was a 2.5-fold range of DEX CL values, from 0.130 to 0.300 L/h/kg, with a mean CL of 0.173 L/h/kg and mean V_{ss} of 1.06 L/kg in man. Our recent study in Indian women applied

LC-MS/MS analysis with extended sampling times (96 h) that revealed a later and slower terminal phase in DEX disposition than that found in earlier studies (Jobe et al., 2020; Krzyzanski et al., 2021), but the apparent CL value was similar (0.160 L/h/kg) to the mean of all studies.

4.3 | Species comparison of DEX metabolism

There are some species similarities and differences in the metabolism of DEX. The drug forms inactive hydroxylated metabolites mediated by CYP3A4 in human liver with inhibition by ketoconazole (Gentile et al., 1996). However, like cortisol and prednisolone, it also undergoes reversible conversion to the inactive 11-keto metabolite by 11β-hydroxysteroid dehydrogenase (11β-OH-DH) in the human kidney (Diederich et al., 1997; Siebe et al., 1993). About 9% of an IV dose of DEX is excreted unchanged in urine (Miyabo et al., 1981), while 6β-OH-DEX is the main urinary metabolite, accounting for 30% of an IV dose of DEX in man (Minagawa et al., 1986). Rat kidney and rectal tissue also exhibit DEX and 11-keto-DEX interconversion (Siebe et al., 1993). Species comparisons of hepatic microsomal CYP3A activity in the formation of 6β-OH-DEX showed the following rank order: hamster > man > rabbit > rat (male) > guinea pig > mouse (Tomlinson et al., 1997). Interestingly, there was very little CYP3A activity found in female rat liver, consistent with our finding smaller CL values for DEX (Song et al., 2020) and methylprednisolone (Ayyar et al., 2019) in female vs. male rats. About 3% of an IV dose of DEX was collected in the bile of male rats (Ogiso et al., 1985), indicating the possibility of a small degree of enterohepatic circulation of the drug. This is less likely to occur in larger species owing to the molecular weight of DEX (392.5 g/mol). In assessing hepatic microsomal metabolism, unbound intrinsic CL were 3.96 in man and 1.44 L/h/kg in monkeys (Akabane et al., 2010); in vivo CL values were more similar (Tables 3 and 4).

The most common pathway of drug metabolism is mediated by CYP3A and it is thus of interest whether our findings reflect a general pattern of species similarities and differences. The PK of several probe substrates of various CYP pathways were examined in six species (Sakai et al., 2015). While they did not perform allometric scaling, the values of total CL (IV dosing) and intrinsic CL (in vitro metabolism) of the classic CYP3A substrate, midazolam were reported. An allometric plot of these values is shown in Figure S1. It can be seen that the allometric relationships are similar to DEX, with comparable b and r^2 values. A review of species differences in CYP-mediated drug metabolism in mouse, rat, dog, monkey, and man describes varying isoforms of CYP3A in these species that show different substrate specificities, “making the extrapolation from animal to man quite hazardous” (Martignoni et al., 2006, p. 886). This is obviated in current drug development by the use of human microsomes and hepatocytes in the preclinical assessment of drug metabolic rates and pathways, albeit with imperfect in vivo predictability (Wood et al., 2017).

4.4 | Study limitations

This review and meta-analysis utilized all available PK studies of DEX that could be found in PubMed and by reference tracing. There are some limitations in this study owing to the assumptions and data sources. The blood:plasma ratio is 0.72 in rat (Song et al., 2020), 1.34 in monkey, and 0.95 in man (Akabane et al., 2010), which may be a source of some species

differences when using plasma concentrations. Plasma protein binding values were available for only some species, albeit all were similar (Table 3), including an f_u value of 0.175 in our recent PBPK rat study (Song et al., 2020). DEX is a substrate of P-gp (Schinkel et al., 1995; Ueda et al., 1992) and efflux from some tissues such as brain may vary with species and alter K_p and V_{ss} values (Kawahara et al., 1999). The early published studies employed RIA assays, later high-performance liquid chromatography methods were implemented, and recently LC-MS/MS was used with much improved sensitivity (Song et al., 2020). Finally, most PK data used in this study are IV single-dose profiles digitized from the literature and discrepancies were found between numerical values reported in published tables and values found or recalculated by NCA and fitting when regenerating mean PK profiles (Table 3). This was especially so for pig and rabbit. The methods of fitting PK profiles and generating CL and V_{ss} values also vary among studies and we sometimes found some variability in using different fitting approaches (Supporting Information Materials). All of these issues compound the difficulties in reviewing the literature and attempting a meta-analysis.

5 | CONCLUSIONS

We collected PK profiles from 11 species for DEX, an important therapeutic agent for veterinary and human use, and utilized traditional basic allometric assessments along with mPBPK and a2CM joint fitting of all available data. While DEX exhibits reasonable (for allometry), but imperfect, scaling of CL to BW, its distribution kinetics appear consistent in most species. While the mPBPK and a2CM approaches produce similar fittings across species, we argue that the mPBPK model requires fewer fitted parameters and offers better clarity in the interpretation of fitted parameters. This study provides a systematic review and analysis of DEX PK in all available species, describes some limitations in synthesizing literature sources, and demonstrates efficiencies and advantages in fitting data across species using generalized physiological parameters and joint fitting methods.

Supplementary Material

Refer to Web version on PubMed Central for supplementary material.

ACKNOWLEDGMENT

This research was supported by NIH Grant R35 GM131800.

Funding information

NIH, Grant/Award Number: R35 GM131800

Abbreviations:

a2CM	allometric two-compartment model
DEX	dexamethasone
Kp	tissue/plasma partition coefficient
LC-MS/MS	liquid chromatography with mass spectroscopy/mass spectroscopy

mPBPK	minimal physiologically-based pharmacokinetic
NCA	noncompartmental analysis
PBPK	physiologically-based pharmacokinetics

REFERENCES

Akabane T, Tabata K, Kadono K, Sakuda S, Terashita S, & Teramura T (2010). A comparison of pharmacokinetics between humans and monkeys. Drug Metabolism & Disposition, 38(2), 308–316. [PubMed: 19910513]

Al Katheeri NA, Wasfi IA, Lambert M, & Saeed A (2004a). Pharmacokinetics and pharmacodynamics of dexamethasone after intravenous administration in camels: Effect of dose. Veterinary Research Communications, 28, 525–542. [PubMed: 15509026]

Al Katheeri NA, Wasfi IA, Lambert M, & Saeed A (2004b). Lack of gender effect on the pharmacokinetics and pharmacodynamics of dexamethasone in the camel after intravenous administration. Research in Veterinary Science, 77, 73–81. [PubMed: 15120956]

Ayyar VS, DuBois DC, Nakamura T, Almon RR, & Jusko WJ (2019). Modeling corticosteroid pharmacokinetics and pharmacodynamics—II: Sex differences in methylprednisolone pharmacokinetics and corticosterone suppression. Journal of Pharmacology and Experimental Therapeutics, 370, 327–336.

Bahar FG, Ohura K, Ogihara T, & Imai T (2012). Species difference of esterase expression and hydrolase activity in plasma. Journal of Pharmaceutical Sciences, 101(10), 3979–3988. [PubMed: 22833171]

Balis FM, Lester CM, Chrousos GP, Heideman RL, & Poplack DG (1987). Differences in cerebrospinal fluid penetration of corticosteroids: Possible relationship to the prevention of meningeal leukemia. Journal of Clinical Oncology, 5, 202–207. [PubMed: 3806166]

Banerjee S, & Bhattacharjee RC (1963). Distribution of body water in the camel (*Camelus dromedaries*). American Journal of Physiology, 204, 1045–1047.

Boxenbaum H (1982). Allometry, physiological time, and the ground plan of pharmacokinetics. Journal of Pharmacokinetics and Biopharmaceutics, 10, 201–227. [PubMed: 7120049]

Boxenbaum H, & Fertig JB (1984). Scaling of antipyrine intrinsic clearance of unbound drug in 15 mammalian species. European Journal of Drug Metabolism and Pharmacokinetics, 9, 177–183. [PubMed: 6745307]

Braat MC, Oosterhuis B, Koopmans RP, Meewis JM, & Van Boxtel CJ (1992). Kinetic-dynamic modeling of lymphocytopenia induced by the combined action of dexamethasone and hydrocortisone in humans, after inhalation and intravenous administration of dexamethasone. Journal of Pharmacology and Experimental Therapeutics, 262, 509–515.

Brightman FA, Leahy DE, Searle GE, & Thomas S (2006). Application of a generic physiologically-based pharmacokinetic model to the estimation of xenobiotic levels in human plasma. Drug Metabolism & Disposition, 34, 94–101. [PubMed: 16221756]

Brown RP, Delp MD, Lindstedt SL, Rhomberg LR, & Beliles RP (1997). Physiological parameter values for physiologically-based pharmacokinetic models. Toxicology and Industrial Health, 13, 407–484. [PubMed: 9249929]

Cao Y, & Jusko WJ (2012). Applications of minimal physiologically-based pharmacokinetic models. Journal of Pharmacokinetics and Pharmacodynamics, 39, 711–723. [PubMed: 23179857]

Charles B, Schild P, Steer P, Cartwright D, & Donovan T (1993). Pharmacokinetics of dexamethasone following single-dose intravenous administration to extremely low birth weight infants. Developmental Pharmacology and Therapeutics, 20, 205–210. [PubMed: 7828455]

Cunningham FE, Rogers S, Fischer JH, & Jensen RC (1996). The pharmacokinetics of dexamethasone in the Thoroughbred racehorse. Journal of Veterinary Pharmacology and Therapeutics, 19, 68–71. [PubMed: 8992029]

Diederich S, Hanke B, Oelkers W, & Bahr V (1997). Metabolism of dexamethasone in the human kidney: Nicotinamide adenine dinucleotide-dependent 11beta-reduction. The Journal of Cinical Endocrinology and Metabolism, 82, 1598–1602.

Duggan DE, Yeh KC, Matalia N, Ditzler CA, & McMahon FG (1975). Bioavailability of oral dexamethasone. Clinical Pharmacology & Therapeutics, 18, 205–209. [PubMed: 1097154]

D'Argenio DZ, & Schumizky A (2009). ADAPT 5 user's guide: Pharmacokinetic/pharmacodynamics systems analysis software. Los Angeles: Biomedical Simulations Resource.

Gentile DM, Tomlinson ES, Maggs JL, Park K, & Back DJ (1996). Dexamethasone metabolism by human liver in vitro. Metabolite identification and inhibition of hydroxylation. Journal of Pharmacology and Experimental Therapeutics, 277, 105–112.

Greco DS, Brown SA, Gauze JJ, Wetse DW, & Buck JM (1993). Dexamethasone pharmacokinetics in clinically normal dogs during low- and high-dose dexamethasone suppression testing. American Journal of Veterinary Research, 54, 580–585. [PubMed: 8387253]

Hall C, Lueshen E, Mosat A, & Linninger AA (2012). Interspecies scaling in pharmacokinetics: A novel whole-body physiologically-based modeling framework to discover drug biodistribution mechanisms in vivo. Journal of Pharmaceutical Sciences, 101, 1221–1241. [PubMed: 22105643]

Hare LE, Yeh KC, Ditzler CA, McMahon FG, & Duggan DE (1975). Bioavailability of dexamethasone II. Dexamethasone phosphate. Clinical Pharmacology & Therapeutics, 18, 330–337. [PubMed: 1100302]

Haspel AD, Giguere S, Hart KA, Berghaus LJ, & Davis JL (2018). Bioavailability and tolerability of nebulised dexamethasone sodium phosphate in adult horses. Equine Veterinary Journal, 50, 85–90. [PubMed: 28719014]

Hochhaus G, Barth J, Al-Fayoumi S, Suarez S, Derendorf H, Hochhaus R, & Mollmann H (2001). Pharmacokinetics and pharmacodynamics of dexamethasone sodium-m-sulfobenzoate (DS) after intravenous and intramuscular administration: A comparison with dexamethasone phosphate (DP). The Journal of Clinical Pharmacology, 41, 425–434. [PubMed: 11304899]

Huh Y, Smith DE, & Feng MR (2011). Interspecies scaling and prediction of human clearance: Comparison of small- and macro-molecule drugs. Xenobiotica, 41, 972–987. [PubMed: 21892879]

Jia M, Deng C, Luo J, Zhang P, Sun X, Zhang Z, & Gong T (2018). A novel dexamethasone-loaded liposome alleviates rheumatoid arthritis in rats. International Journal of Pharmaceutics, 540, 57–64. [PubMed: 29408684]

Jobe AH, Milad MA, Peppard T, & Jusko WJ (2020). Pharmacokinetics and pharmacodynamics of intramuscular and oral betamethasone and dexamethasone in reproductive age women in India. Clinical and Translational Science, 13, 391–399. [PubMed: 31808984]

Kawahara M, Sakata A, Miyashita T, Tamai I, & Tsuji A (1999). Physiologically-based pharmacokinetics of digoxin in mdr1a knockout mice. Journal of Pharmaceutical Sciences, 88, 1281–1287. [PubMed: 10585223]

Ke AB, & Milad MA (2019). Evaluation of maternal drug exposure following the administration of antenatal corticosteroids during late pregnancy using physiologically-based pharmacokinetic modeling. Clinical Pharmacology & Therapeutics, 106, 164–173. [PubMed: 30924921]

Kitagawa H, Mohri T, & Kitagawa M (1972). Comparative studies on anti-inflammatory effect and biological fates of 21-phosphates and -sulfates of dexamethasone and prednisolone. Arzneimittel Forschung, 22, 402–410. [PubMed: 5067495]

Knych HK, Weiner D, Arthur RM, Baden R, McKemie DS, & Kass PH (2020). Serum concentrations, pharmacokinetic/pharmacodynamic modeling and effects of dexamethasone on inflammatory mediators following intravenous and oral administration to exercised horses. Drug Testing and Analysis, 12, 1087–1101. [PubMed: 32436346]

Kotula AW, & Helbacka NV (1966). Blood volume of live chickens and influence of slaughter technique on blood loss. Poultry Science, 45, 684–688.

Krzyzanski W, Milad MA, Jobe AH, Peppard T, Bies RR, & Jusko WJ (2021). Population pharmacokinetic modeling of intramuscular and oral dexamethasone and betamethasone in Indian women. Journal of Pharmacokinetics and Pharmacodynamics, 48.

Lepist E-I, & Jusko WJ (2004). Modeling and allometric scaling of s(+) ketoprofen pharmacokinetics and pharmacodynamics: A retrospective analysis. Journal of Veterinary Pharmacology and Therapeutics, 27, 211–218. [PubMed: 15305849]

Li L, Li Z, Deng C, Ning M, Li H, Bi S, Zhou T, & Lu W (2012). A mechanism-based pharmacokinetic/pharmacodynamic model for CYP3A1/2 induction by dexamethasone in rats. Acta Pharmacologica Sinica, 33, 127–136. [PubMed: 22212433]

Loew D, Schuster O, & Graul EH (1986). Dose-dependent pharmacokinetics of dexamethasone. European Journal of Clinical Pharmacology, 30, 225–230. [PubMed: 3709651]

Mager DE, Lin SX, Blum RA, Lates CD, & Jusko WJ (2003). Dose equivalency evaluation of major corticosteroids: Pharmacokinetics and cell trafficking and cortisol dynamics. The Journal of Clinical Pharmacology, 43, 1216–1227. [PubMed: 14551176]

Mahmood I (1998). Integration of in vitro data and brain weight in allometric scaling to predict clearance in humans: Some suggestions. Journal of Pharmaceutical Sciences, 87, 527–528. [PubMed: 9548910]

Martignoni M, Groothuis GM, & de Kanter R (2006). Species differences between mouse, rat, dog, monkey and human CYP-mediated drug metabolism, inhibition and induction. Expert Opinion on Drug Metabolism and Toxicology, 2, 875–894. [PubMed: 17125407]

Meno-Tetang GM, Li H, Mis S, Pyszczynski N, Heining P, Lowe P, & Jusko WJ (2006). Physiologically-based pharmacokinetic modeling of FTY720 (2-amino-2[2-(−4-octylphenyl)ethyl]propane-1,3-diol hydrochloride) in rats after oral and intravenous doses. Drug Metabolism and Disposition, 34, 1480–1487. [PubMed: 16751263]

Minagawa R, Kasuya Y, Baba S, Knapp G, & Skelly JP (1986). Identification and quantification of 6β-hydroxy-dexamethasone as a major urinary metabolite of dexamethasone in man. Steroids, 47, 175–188. [PubMed: 3564085]

Miyabo S, Nakamura T, Kuwazima S, & Kishida S (1981). A comparison of the bioavailability and potency of dexamethasone phosphate and sulphate in man. European Journal of Clinical Pharmacology, 20, 277–282. [PubMed: 6273180]

O'Sullivan BT, Cutler DJ, Hunt GE, Walters C, Johnson GF, & Caterson ID (1997). Pharmacokinetics of dexamethasone and its relationship to dexamethasone suppression test outcome in depressed patients and healthy control subjects. Biological Psychiatry, 41, 574–584. [PubMed: 9046990]

Ogiso T, Iwaki M, & Ohtori A (1985). Effect of dicyclomine on intestinal absorption, disposition and biliary excretion of dexamethasone. Journal of Pharmacobio-Dynamics, 8, 41–49. [PubMed: 4009396]

Peets EA, Staub M, & Symchowicz S (1969). Plasma binding of betamethasone-3H, dexamethasone-3H, and cortisol-14C—A comparative study. Biochemical Pharmacology, 18, 1655–1663. [PubMed: 5817301]

Riviere JE, Martin-Jimenez T, Sundlof SF, & Craigmill AL (1997). Interspecies allometric analysis of the comparative pharmacokinetics of 44 drugs across veterinary and laboratory animal species. Journal of Veterinary Pharmacology and Therapeutics, 20, 453–463. [PubMed: 9430769]

Rodionov N (2000). Graph digitizer version 1.9 http://www.geocities.com/graphdigitizer/

Rohdewald P, Mollmann H, Barth J, Rehder J, & Derendorf H (1987). Pharmacokinetics of dexamethasone and its phosphate ester. Biopharmaceutics & Drug Disposition, 8, 205–212. [PubMed: 3593899]

Rose JQ, Yurchak AM, Meikle AW, & Jusko WJ (1981). Effect of smoking on prednisone, prednisolone, and dexamethasone pharmacokinetics. Journal of Pharmacokinetics and Biopharmaceutics, 9, 1–14. [PubMed: 7229914]

Sakai C, Iwano S, Yamazaki Y, Ando A, Nakane F, Kouno M, Yamazaki H, & Miyamoto Y (2015). Species differences in the pharmacokinetic parameters of cytochrome P450 probe substrates between experimental animals, such as mice, rats, dogs, monkeys, and microminipigs, and humans. Journal of Drug Metabolism & Toxicology, 5, 1–12.

Samtani MN, & Jusko WJ (2005a). Comparison of dexamethasone pharmacokinetics in female rats after intravenous and intramuscular administration. Biopharmaceutics & Drug Disposition, 26, 85–91. [PubMed: 15654687]

Samtani MN, & Jusko WJ (2005b). Stability of dexamethasone sodium phosphate in rat plasma. International Journal of Pharmaceutics, 301, 262–266. [PubMed: 16054309]

Schinkel AH, Wagenaar E, Van Deemter L, Mol CA, & Borst P (1995). Absence of the mdr1a P-Glycoprotein in mice affects tissue distribution and pharmacokinetics of dexamethasone, digoxin, and cyclosporine A. Journal of Clinical Investigation, 96, 1698–1705.

Schmidt AF, Jobe AH, Kannan PS, Bridges JP, Newnham JP, Saito M, Usuda H, Kumagai Y, Fee EL, Clarke M, & Kemp MW (2019). Oral antenatal corticosteroids evaluated in fetal sheep. Pediatric Research, 86, 589–594. [PubMed: 31365919]

Siebe H, Baude G, Lichtenstein I, Wang D, Buhler H, Hoyer GA, & Heirholzer K (1993). Metabolism of dexamethasone: Sites and activity in mammalian tissues. Renal Physiology and Biochemistry, 16, 79–88. [PubMed: 7684150]

Soma LR, Uboh CE, Liu Y, Li X, Robinson MA, Boston RC, & Colahan PT (2013). Pharmacokinetics of dexamethasone following intra-articular, intravenous, intramuscular, and oral administration in horses and its effects on endogenous hydrocortisone. Journal of Veterinary Pharmacology and Therapeutics, 36, 181–191. [PubMed: 22632064]

Soma LR, Uboh CE, Luo Y, Guan F, Moate PJ, & Boston RC (2005). Pharmacokinetics of dexamethasone with pharmacokinetic/pharmacodynamic model of the effect of dexamethasone on endogenous hydrocortisone and cortisone in the horse. Journal of Veterinary Pharmacology and Therapeutics, 28, 71–80. [PubMed: 15720518]

Song D, Sun L, DuBois DC, Almon RR, Meng S, & Jusko WJ (2020). Physiologically-based pharmacokinetics of dexamethasone in rats. Drug Metabolism Disposition, 48, 811–818. [PubMed: 32601175]

Tang H, & Mayersohn M (2005). A novel model for prediction of human drug clearance by allometric scaling. Drug Metabolism & Disposition, 33, 1297–1303. [PubMed: 15958605]

Tomlinson ES, Maggs JL, Park BK, & Back DJ (1997). Dexamethasone metabolism in vitro: Species differences. The Journal of Steroid Biochemistry and Molecular Biology, 62, 345–352. [PubMed: 9408089]

Toutain PL, Alvinerie M, & Ruckebusch Y (1983). Pharmacokinetics of dexamethasone and its effect on adrenal gland function in the dog. American Journal of Veterinary Research, 44, 212–217. [PubMed: 6830010]

Toutain PL, Brandon RA, Alvinerie M, Garcia-Villar R, & Ruckebusch Y (1982). Dexamethasone in cattle: Pharmacokinetics and action on the adrenal gland. Journal of Veterinary Pharmacology and Therapeutics, 5, 33–43. [PubMed: 7097848]

Toutain PL, Brandon RA, de Pomyers H, Alvineri M, & Baggot JD (1984). Dexamethasone and prednisolone in the horse: Pharmacokinetics and action on the adrenal gland. American Journal of Veterinary Research, 45, 1750–1756. [PubMed: 6497132]

Trenque T, Lamiable D, Vistelle R, Millart H, Leperr A, & Choisy H (1994). Comparative pharmacokinetics of two diastereoisomers dexamethasone and betamethasone in plasma and cerebrospinal fluid in rabbits. Fundamental & Clinical Pharmacology, 8, 430–436. [PubMed: 7875637]

Tsuei SE, Moore RG, Ashley JJ, & McBride WG (1979). Disposition of synthetic glucocorticoids. I. Pharmacokinetics of dexamethasone in healthy adults. Journal of Pharmacokinetics and Biopharmaceutics, 7, 249–264. [PubMed: 480147]

Ueda K, Okamura N, Hirai M, Tanigawara Y, Saeki T, Kioka N, Komano T, & Hori R (1992). Human P-glycoprotein transports cortisol, aldosterone, and dexamethasone, but not progesterone. Journal of Biological Chemistry, 267, 24248–24252.

Varma DR, & Mulay S (1980). Anti-inflammatory and ulcerogenic effects and pharmacokinetics of dexamethasone in protein-deficient rats. Journal of Pharmacology and Experimental Therapeutics, 214, 197–202.

Wang Q, Jiang J, Chen W, Jiang H, Zhang Z, & Sun X (2016). Targeted delivery of low-dose dexamethasone using PCL-PEG micelles for effective treatment of rheumatoid arthritis. Journal of Controlled Release, 230, 64–72. [PubMed: 27057749]

Watteyn A, Wyns H, Plessers E, Russo E, De Baere S, De Backer P, & Croubels S (2013). Pharmacokinetics of dexamethasone after intravenous and intramuscular administration in broiler chickens. The Veterinary Journal, 195, 216–220. [PubMed: 22835862]

Wolfensohn S, & Lloyd M (2003). Handbook of laboratory animal management and welfare (3rd ed.). Wiley-Blackwell.

Wood FL, Houston JB, & Hallifax D (2017). Clearance prediction methodology needs fundamental improvement: Trends common to rat and human hepatocytes/microsomes and implications for experimental methodology. Drug Metabolism & Disposition, 45, 1178–1188. [PubMed: 28887366]

Workman RJ, Vaughn WK, & Stone WJ (1986). Dexamethasone suppression testing in chronic renal failure: Pharmacokinetics of dexamethasone and demonstration of a normal hypothalamic-pituitary-adrenal axis. The Journal of Cinical Endocrinology and Metabolism, 63, 741–746.

Wyns H, Meyer E, Watteyn A, Plessers E, De Baere S, De Backer P, & Croubels S (2013). Pharmacokinetics of dexamethasone after intravenous and intramuscular administration in pigs. The Veterinary Journal, 198, 286–288. [PubMed: 23876308]

Yuan Y, Zhou X, Li J, Ye S, Ji X, Li L, Zhou T, & Lu W (2015). Development and validation of a highly sensitive LC-MS/MS method for the determination of dexamethasone in nude mice plasma and its application to a pharmacokinetic study. Biomedical Chromatography, 29, 578–583. [PubMed: 25165023]

Zhao J, Cao Y, & Jusko WJ (2015). Across-species scaling of monoclonal antibody pharmacokinetics using a minimal PBPK model. Pharmaceutical Research, 32, 3269–3281. [PubMed: 25939552]

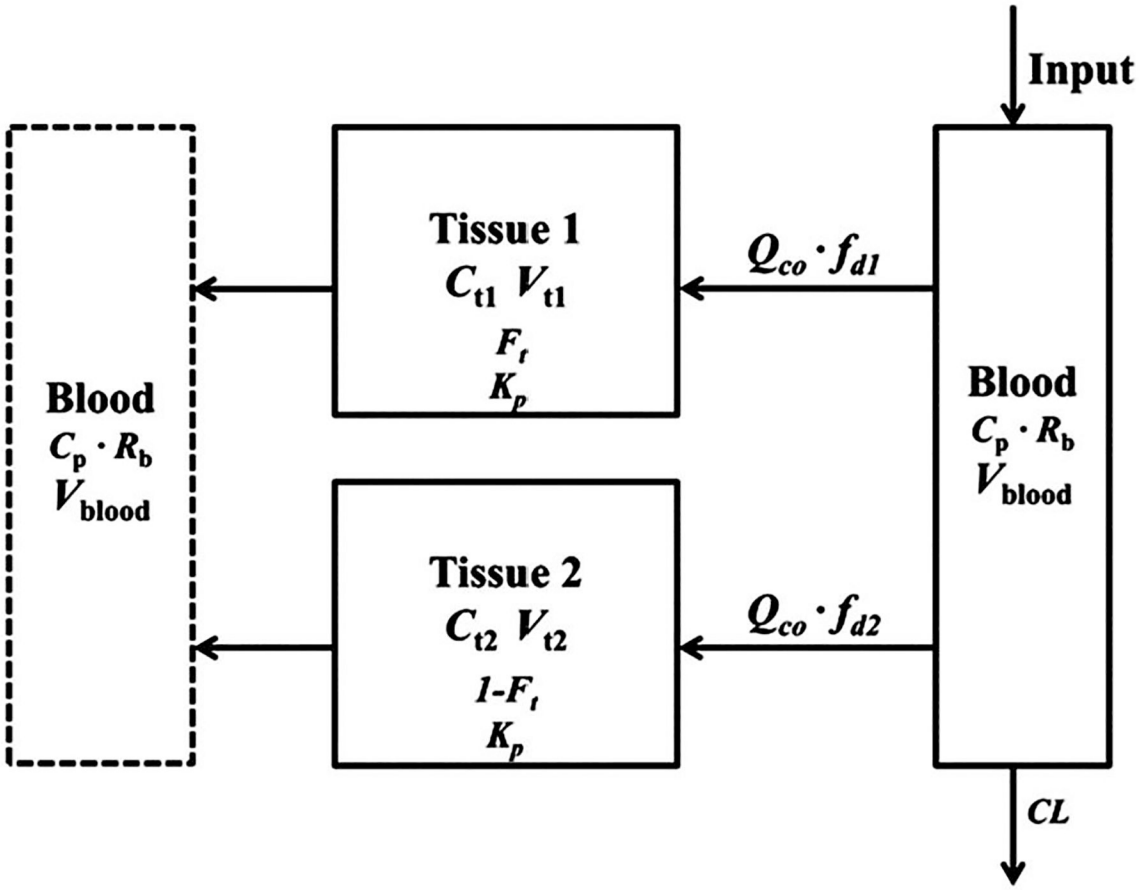

FIGURE 1.

The minimal physiologically-based pharmacokinetic model with two tissue compartments (single K_p). Blood flow and physiological volumes are used to characterize the distribution spaces and connections among tissue and blood compartments. Symbols are defined in Table 1

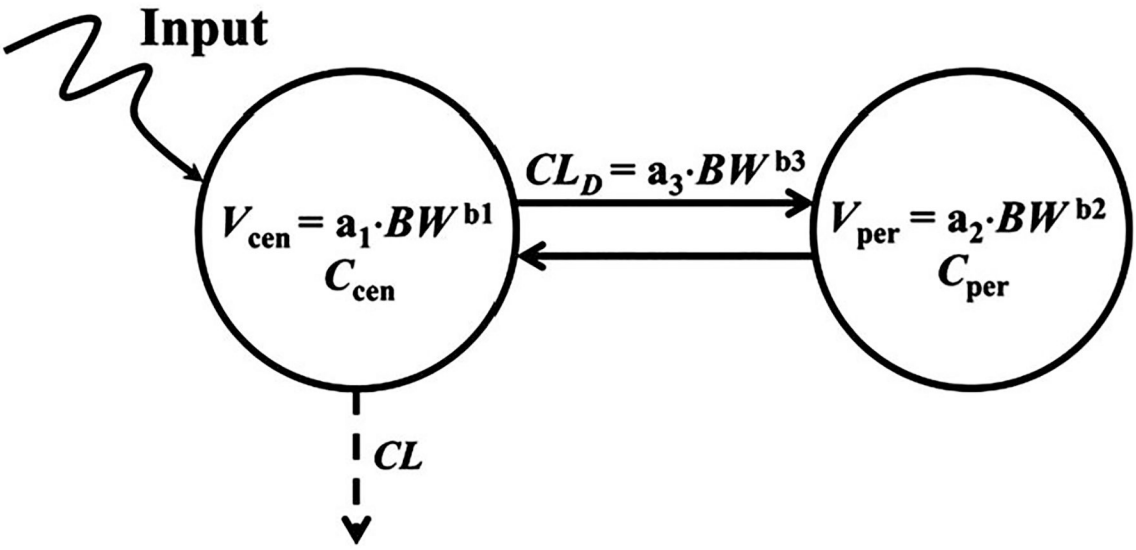

FIGURE 2.

The two-compartment pharmacokinetic model with allometric scaling of all parameters. Allometric equations are used to represent volumes and distribution clearance. Symbols are defined in Table 2

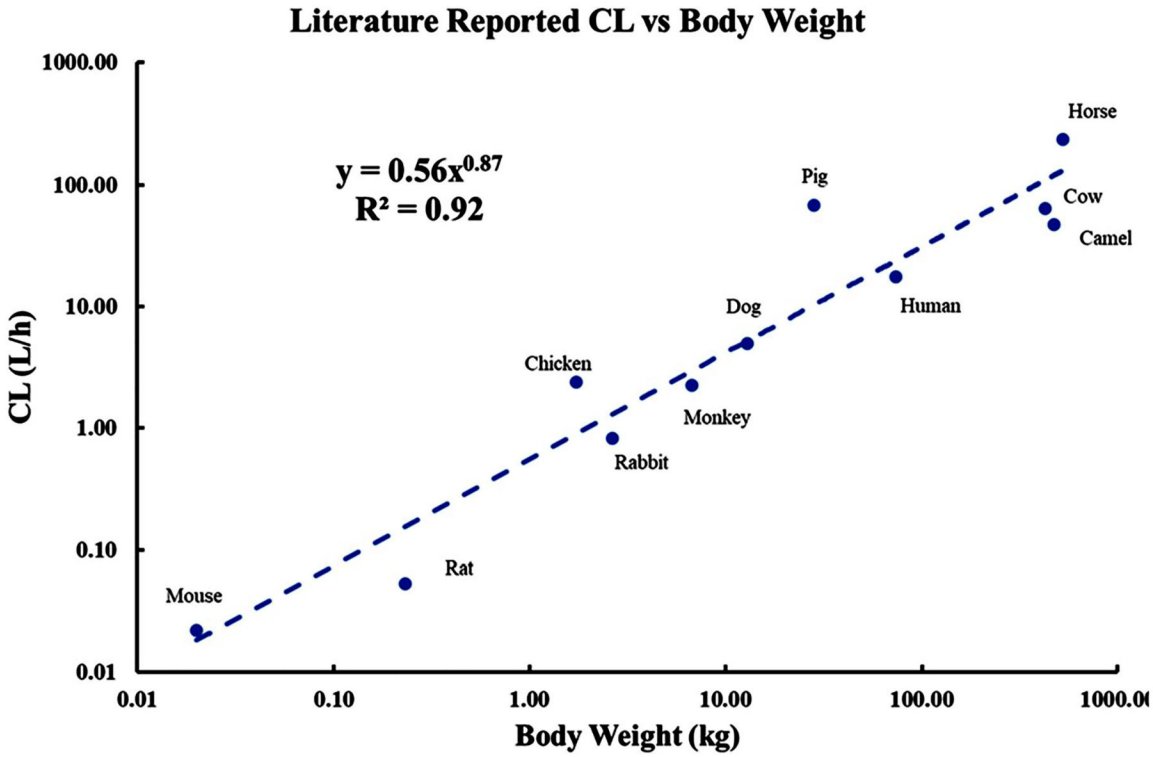

FIGURE 3.

Allometric relationship between literature reported clearances (Table 3) and body weights of 11 species. The regression line was fitted by the indicated power equation

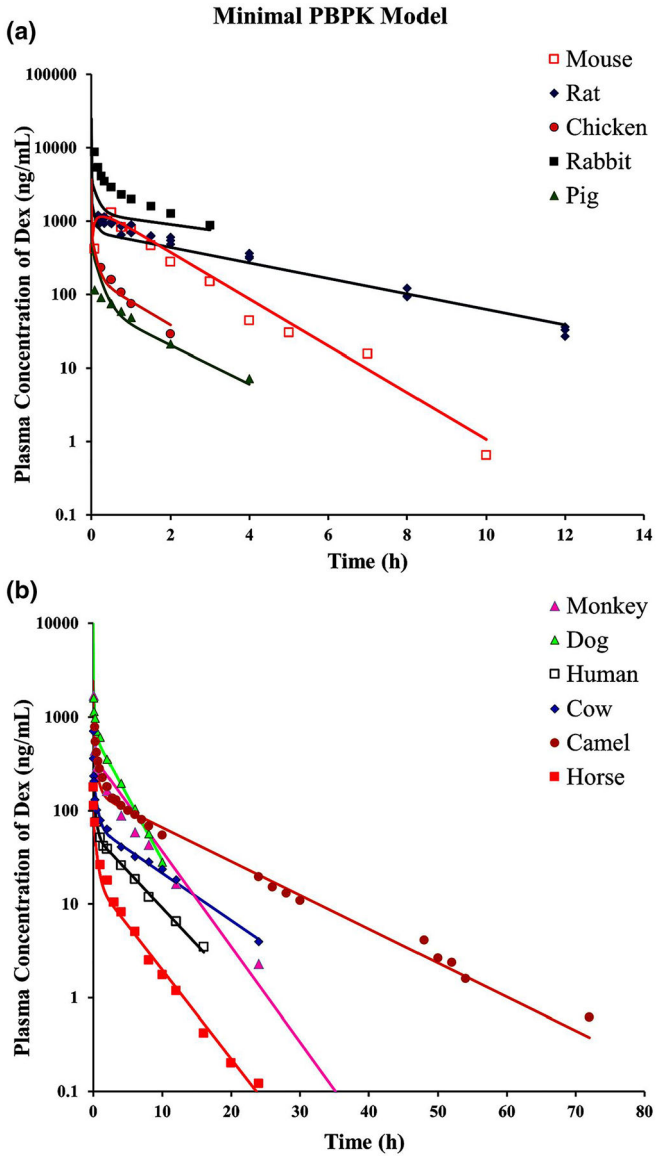

FIGURE 4.

The fitting of dexamethasone pharmacokinetic profiles of 11 species using the minimal physiologically-based pharmacokinetic model (Figure 1). Symbols and fitted parameters are listed in Table 1. (a) Fitted profiles of rat, rabbit, pig, chicken, and mice. (b) Fitted profiles of cow, horse, dog, camel, human, and monkey. The pharmacokinetic profiles from different species are graphed on two panels to allow visual separation of data and fittings

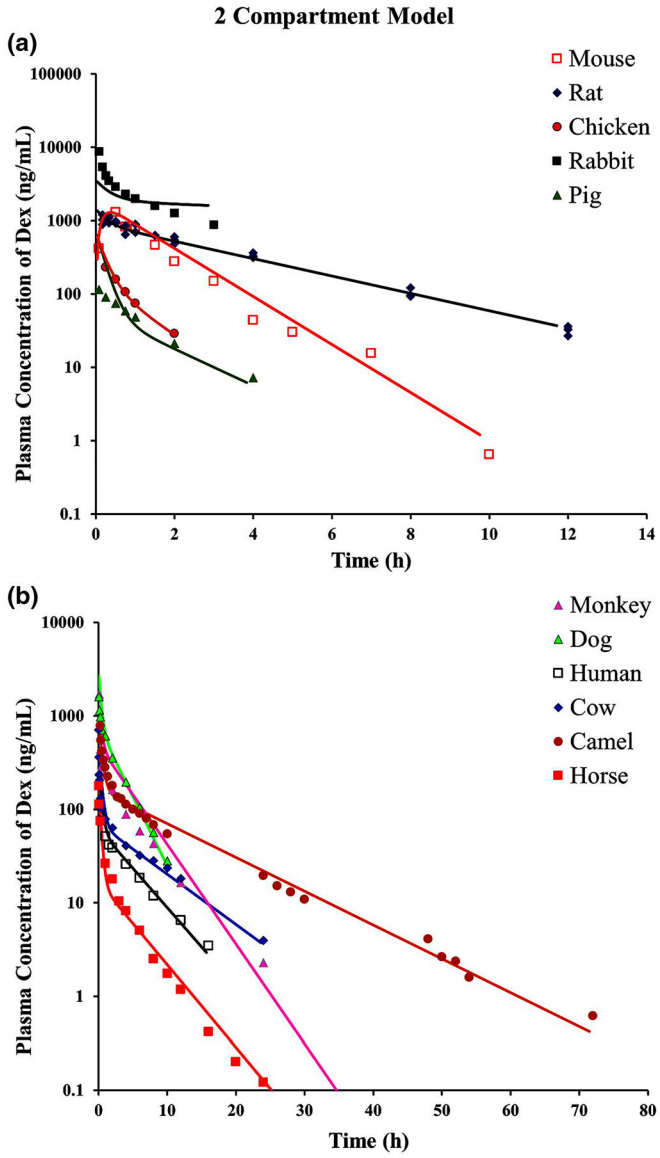

FIGURE 5.

The fitting of dexamethasone pharmacokinetic profiles of 11 species using the allometric two-compartment model (Figure 2). Symbols and fitted parameters are listed in Table 2. The separate panels are the same as described in Figure 4

TABLE 1

PK parameters of dexamethasone across 11 species using the joint mPBPK[a]

Parameter	Definition	Estimate (CV%)
K_p	Tissue to plasma partition coefficient	1.07 (1.93)
f_{d1}	Fraction of Q_{CO} for tissue 1	0.85 (1.22)
f_{d2}	Fraction of Q_{CO} for tissue 2	0.15[b]
F_t	Fraction of total tissue volume for tissue 1	0.26 (7.50)
F	Bioavailability of intraperitoneal dose in mouse	0.86 (fixed)
k_a	Absorption rate constant for mice (h^{-1})	5 (fixed)

Note: The jointly fitted CL values are listed in Table 5.

Abbreviations: AIC, Akaike Information Criterion; CL, clearance; CV, coefficient of variation; mPBPK, minimal physiologically-based pharmacokinetic; PK, pharmacokinetic.

[a]AIC = 1410.4.

[b]Secondary parameter: $f_{d2} = 1 - f_{d1}$.

TABLE 2

Pharmacokinetic parameters of dexamethasone across 11 species using the joint a2CM with scaling of distribution parameters[a]

Parameter	Definition	Estimates (CV%)
a_1	Scaling intercept for V_{cen}	1.12 (14.76)
b_1	Scaling exponent for V_{cen}	0.88 (1.77)
a_2	Scaling intercept for V_{per}	0.13 (27.18)
b_2	Scaling exponent for V_{per}	1.13 (2.00)
a_3	Scaling intercept for CL_D	1.02 (52.85)
b_3	Scaling exponent for CL_D	0.92 (4.82)
F	Bioavailability of intraperitoneal dose	0.86 (fixed)
k_a	Absorption rate constant for mouse (1/h)	5 (fixed)

Note: The jointly fitted CL values are listed in Table 5.

Abbreviations: AIC, Akaike Information Criterion; a2CM, allometric two-compartment model; CL, clearance; CV, coefficient of variation.

[a]AIC = 1422.9.

TABLE 3

Literature reports and calculations of pharmacokinetic parameters of dexamethasone for different species

Reference	Species	Weight (kg)	Unbound (%)	Dosing route	Dose[a] (mg/kg)	Reported CL (L/h/kg)	Reported V_{ss} (L/kg)	NCA CL (L/h/kg)	NCA V_{ss} (L/kg)	Allometric regression CL (L/h/kg)
Yuan et al. (2015) [b]	Mouse	0.02		IP	2.00	1.11[c]	1.46[c]	1.10	1.42	0.92
Varma and Mulay (1980)	Rat		17.0	IV	2.00	0.18	0.97			
Ogiso et al. (1985)	Rat			IV	1.52	0.34	1.19			
Samtani and Jusko (2005a, 2005b) [b]	Rat	0.23	15.3[d]	IV	0.83	0.23	0.78	0.22	0.75	0.67
Wang et al. (2016) [e]	Rat			IV	0.25	0.22	0.86			
Jia et al. (2018) [e]	Rat			IV	1.00	0.22	0.72			
Watteyn et al. (2013) [b]	Chicken	1.73		IV	0.30	1.38	0.93	1.17	1.00	0.52
Trenque et al. (1994) [b]	Rabbit	2.65	21.9	IV	1.52	0.31	0.63	0.17	0.36	0.49
Wyns et al. (2013) [b]	Pig	28.3		IV	0.23	2.39	2.12[e]	1.50	2.12	0.36
Toutain et al. (1983) [b]	Dog	13.0	27.3[d]	IV	1.00	0.38	1.07[f]	0.39	1.05	0.40
Greco et al. (1993)	Dog			IV	0.10	0.58	3.13[f]			
Balis et al. (1987) [b]	Monkey	6.75	30.0	IV	0.50[g]	0.33[g]	1.21[g]	0.33	1.18	0.44
Akabane et al. (2010)	Monkey			IV	0.25	0.27	NA			
Mager et al. (2003) [b]	Man	73.6	22.6[d]	IV	0.08	0.24	1.19[e]	0.24	1.25	0.32
Toutain et al. (1982) [b]	Cow	425	26.2[d]	IV	0.10	0.15	1.13[f]	0.14	0.99	0.26
Al Katheeri et al. (2004a, 2004b) [b]	Camel	475	25.0	IV	0.20	0.10	1.13	0.08	0.70	0.25
Al Katheeri et al. (2004a, 2004b)	Camel			IV	0.05	0.11	0.80			
Cunningham et al. (1996)	Horse			IV	0.023	0.48	1.73			
Soma et al. (2005)	Horse			IV	0.05	0.44	2.10			
Soma et al. (2013) [b]	Horse	524		IV	0.038	0.45	1.60	0.26	0.72	0.25
Haspel et al. (2018)	Horse			IV	0.007	0.46	2.18[f]			
Knych et al. (2020)	Horse			IV	0.056	0.47	1.86			

Abbreviations: 2CM, two-compartment model; CL, clearance; DEX, dexamethasone; NCA, noncompartmental analysis; PK, pharmacokinetic.

[a] Dose expressed as DEX-free alcohol when DEX sodium phosphate given.

[b] Dataset used for minimal physiologically-based pharmacokinetic and 2CM model fitting across 11 species.

[c] Due to IP injection, CL/F and V_{SS}/F are shown here.

[d] Percent unbound values are from Peets et al. (1969).

[e] Plasma concentration–time profiles in the literature were digitized and NCA used to calculate PK parameters.

[f] Calculated based on PK parameters reported in the literature.

[g] Converted from per body surface (m^2) to per body weight (kg).

TABLE 4

Summary of literature data for the pharmacokinetics of dexamethasone in man

Reference	Subjects Sex	Type of subjects	Assay method	Dosing route	Dose (mg)	CL (L/h/kg)	V_{ss} (L/kg)
Duggan et al. (1975)	11 M	Healthy	RIA	IV	12	0.130	
Hare et al. (1975)	9	Healthy	RIA	IV	1 mg/kg	0.168	
Tsuei et al. (1979)	6 F, 6 M	Healthy	HPLC	IV	6.66	0.210	0.75
Rose et al. (1981)	8 M	Healthy	RIA	IV	4	0.177	1.08
Miyabo et al. (1981)	10 M	Healthy	RIA	IV	20	0.188	
Loew et al. (1986)	10 F	Healthy	RIA	IM	3	0.141	1.00
Workman et al. (1986)	6	Healthy	RIA	IV	1	0.111	0.58
Rohdewald et al. (1987)	7 M, 3 F	Healthy	RIA	IV	15	0.079	1.20
Braat et al. (1992)	10 M	Healthy	HPLC	IV	3.8	0.300	1.32
O'Sullivan et al. (1997)	5 M, 5 F	Healthy	RIA	IV	1	0.108	0.64
Hochhaus et al. (2001)	10 M	Healthy	RIA	IV	8.3	0.225	1.40
Mager et al. (2003)	5 M	Healthy	HPLC	IV	6	0.247	1.50
Jobe et al. (2020)	12 F	Healthy	LC-MS/MS	IM	6	0.160	1.18

Abbreviations: CL, clearance; F, female; HPLC, high-performance liquid chromatography; LC-MS/MS, liquid chromatography with mass spectroscopy/mass spectroscopy; M, male; RIA, radioimmunoassay.

TABLE 5

Comparison of clearance values of DEX for 11 species based on indicated methods of calculation (CV% obtained by fitting)

Species	Reported CL (L/h/kg)	NCA CL (L/h/kg)	mPBPK joint CL (L/h/kg)	mPBPK individual CL (L/h/kg)	2CM joint CL (L/h/kg)	2CM individual CL (L/h/kg)
Mouse	1.11	1.10	0.84 (3.75)	1.00 (88.50)	0.77 (5.40)	1.00 (7.31)
Rat	0.23	0.22	0.27 (5.10)	0.23 (2.37)	0.24 (2.22)	0.24 (2.35)
Chicken	1.38	1.17	1.01 (8.70)	1.17 (3.86)	1.00 (4.26)	1.26 (4.21)
Rabbit	0.31	0.17	0.19 (97.51)	0.18 (1.84)	0.040 (203)	0.18 (1.84)
Pig	2.39	1.50	1.11 (8.59)	1.21 (8.79)	0.97 (9.73)	1.46 (8.53)
Dog	0.38	0.39	0.39 (2.47)	0.39 (2.07)	0.34 (5.14)	0.40 (2.19)
Monkey	0.33	0.33	0.28 (6.82)	0.34 (5.00)	0.22 (6.96)	0.35 (5.31)
Man	0.24	0.24	0.22 (1.34)	0.23 (1.46)	0.20 (4.41)	0.24 (1.63)
Cow	0.15	0.14	0.14 (3.07)	0.15 (2.80)	0.14 (7.41)	0.14 (5.26)
Camel	0.10	0.08	0.10 (4.19)	0.090 (2.66)	0.090 (3.65)	0.13 (2.70)
Horse	0.45	0.26	0.33 (5.54)	0.27 (2.48)	0.29 (5.00)	0.28 (4.10)

Abbreviations: 2CM, two-compartment models; CL, clearance; DEX, dexamethasone; mPBPK, minimal physiologically-based pharmacokinetic; NCA, noncompartmental analysis.